SUMOylation inhibitor TAK-981 suppresses proliferation and induces apoptosis in SK-UT-1B uterine leiomyosarcoma cells

HOSOUK JOUNG[1] and HYUNJU LIU[1,2]

[1]Department of Obstetrics and Gynecology, Chosun University College of Medicine, Gwangju 61452, Republic of Korea; [2]Department of Obstetrics and Gynecology, Chosun University Hospital, Gwangju 61453, Republic of Korea

Received November 28, 2025; Accepted June 9, 2026

DOI: 10.3892/ol.2026.15724

Abstract. Uterine leiomyosarcoma (Ut-LMS) is an aggressive smooth muscle malignancy with limited therapeutic options and a poor prognosis, underscoring the need for new molecularly-targeted therapies. TAK-981 (subasumstat), a selective inhibitor of small ubiquitin-like modifier (SUMO)-activating enzymes, exhibits antitumor activity in several types of cancer; however, to the best of our knowledge, its therapeutic potential in Ut-LMS has not been explored. The current study evaluated the effects of TAK-981 on human Ut-LMS cells and revealed that SK-UT-1B cells exhibited markedly greater sensitivity to TAK-981 than SK-UT-1 cells. TAK-981 substantially reduced SK-UT-1B cell viability in a time- and concentration-dependent manner, whereas SK-UT-1 cells demonstrated a minimal response to TAK-981 at similar doses. Annexin V staining confirmed that TAK-981 induced the apoptosis of SK-UT-1B cells after 48 h, with apoptotic populations increasing proportionally with drug concentration. Furthermore, TAK-981 induced G_0/G_1 cell cycle arrest and markedly decreased Ki67 expression, indicating suppressed proliferative activity. TAK-981 also triggered substantial intracellular reactive oxygen species (ROS) accumulation and mitochondrial membrane depolarization, and antioxidant co-treatment demonstrated that apoptosis was partially ROS-dependent. Western blotting indicated robust inhibition of SUMO2/3 conjugation and activation of apoptotic markers, including cleaved caspase-3 and poly (ADP-ribose) polymerase, with the upregulation of p21 and p53. By contrast, autophagy markers, such as LC3B and p62, were unchanged, indicating that TAK-981 exerted its cytotoxic effects independently of the autophagic pathway. Collectively, these findings suggested that TAK-981 suppressed proliferation and induced apoptosis in SK-UT-1B Ut-LMS cells, accompanied by SUMOylation inhibition, ROS-associated mitochondrial dysfunction, apoptosis and G_0/G_1 cell-cycle arrest, and may represent a promising therapeutic candidate for further investigation in Ut-LMS.

Correspondence to: Professor Hyunju Liu, Department of Obstetrics and Gynecology, Chosun University College of Medicine, 309 Pilmun-daero, Dong-gu, Gwangju 61452, Republic of Korea
E-mail: lhj@chosun.ac.kr

Abbreviations: Ut-LMS, uterine leiomyosarcoma; SAE, SUMO-activating enzyme; DMSO, dimethyl sulfoxide; LDH, lactate dehydrogenase; ROS, reactive oxygen species; NAC, N-Acetyl-L-cysteine; CAT, catalase; PARP, poly (ADP-ribose) polymerase; SUMO, small ubiquitin-like modifier

Key words: Ut-LMS, TAK-981, SUMOylation, apoptosis, proliferation, SK-UT-1B

Introduction

Although uterine leiomyosarcoma (Ut-LMS) is rare, it is a highly aggressive malignancy arising from the uterine smooth muscle and accounts for less than 1% of all uterine tumors (1,2). Despite its low incidence, Ut-LMS is associated with poor clinical outcomes due to rapid tumor expansion, early hematogenous dissemination, and a high rate of postoperative recurrence (3). Current therapeutic options are limited, with hysterectomy serving as the primary intervention (1). Conventional chemotherapeutic regimens, including doxorubicin, gemcitabine, and docetaxel, offer only modest benefits, and the overall survival of patients with advanced disease has demonstrated little improvement over the last decade (4,5). These challenges highlight the urgent need for new molecular-targeted therapies for Ut-LMS.

Recent genomic and transcriptomic studies have indicated that Ut-LMS harbors substantial molecular heterogeneity and frequently exhibits alterations in TP53, RB1, ATRX, and PTEN with widespread chromosomal instability (6-8). These molecular abnormalities suggest that Ut-LMS cells may rely on stress-adaptive mechanisms that support DNA damage responses, cell-cycle progression, transcriptional regulation, and protein homeostasis. Therefore, targeting regulatory pathways that sustain these adaptive survival mechanisms may provide a rational therapeutic strategy for Ut-LMS.

TAK-981 (subasumstat) is a first-in-class inhibitor of the small ubiquitin-like modifier (SUMO) activation pathway, which functions by covalently inhibiting SUMO-activating enzyme (SAE) complex composed of SAE1 and SAE2 (9,10). SUMOylation is a crucial post-translational modification involved in cell cycle regulation, DNA repair, transcription, and cellular stress responses, and its aberrant regulation can promote tumor progression and therapeutic resistance by supporting oncogenic signaling, genome stability, and

stress-adaptive survival mechanisms in cancer cells (11-13). These functions are particularly relevant to Ut-LMS, which is characterized by frequent alterations in tumor suppressor pathways, chromosomal instability, aggressive proliferation, and therapeutic resistance. Thus, we hypothesized that Ut-LMS cells may be vulnerable to SAE inhibition because blockade of the SUMO pathway could disrupt stress-adaptive mechanisms required for tumor cell survival. Preclinical studies have demonstrated that TAK-981 exerts potent antitumor effects in several malignancies by inducing interferon signaling, apoptosis, and cell cycle arrest (14-16). In addition, our previous study showed that TAK-981 suppressed cell viability and modulated apoptosis, cell-cycle arrest, and autophagy in ELT3 uterine leiomyoma cells (17). Although uterine leiomyoma and Ut-LMS both originate from uterine smooth muscle, they represent biologically distinct benign and malignant tumors, respectively. Therefore, it remains unclear whether the TAK-981-induced cellular responses observed in benign uterine leiomyoma cells can be extended to malignant Ut-LMS cells.

The effects of TAK-981 on cell growth in Ut-LMS cells were investigated and TAK-981 was found to substantially suppress SK-UT-1B cell growth. TAK-981 induced G_0/G_1 cell cycle arrest, triggered reactive oxygen species (ROS)-dependent mitochondrial dysfunction and apoptosis, and inhibited SUMO2/3 conjugation while activating the tumor suppressors, p21 and p53. These findings suggest that targeting the SUMOylation pathway is a novel and promising therapeutic strategy for Ut-LMS.

Materials and methods

Cell culture and reagents. Human Ut-LMS cell lines (SK-UT-1 and SK-UT-1B; ATCC, Manassas, VA, USA) were cultured in the Minimal Essential Medium (LM007-07; Welgene, Gyeongsan, Republic of Korea) supplemented with 10% fetal bovine serum (FBS; SH30919.03; Hyclone, Logan, UT, USA) and 1% penicillin-streptomycin (15140122; Gibco, Waltham, MA, USA) at 37˚C in a humidified atmosphere containing 5% CO_2. TAK-981 (HY-111789; MedChemExpress, Monmouth Junction, NJ, USA) was dissolved in dimethyl sulfoxide (DMSO; DMSO100; LPS Solution, Daejeon, Republic of Korea) and used as vehicle control. N-Acetyl-L-cysteine (NAC; A7250) and catalase (CAT; C1345) were purchased from Sigma-Aldrich (St. Louis, MO, USA).

MTT and lactate dehydrogenase (LDH) assays. Cell viability and cytotoxicity were determined using MTT and LDH assays. Cells were seeded into 96-well plates at a density of $5x10^3$ cells per well and allowed to attach for 24 h before TAK-981 treatment. After exposure to TAK-981 for 24 or 48 h, cell viability was assessed using MTT solution (5 mg/ml; M2128, Sigma-Aldrich, St. Louis, MO, USA). Following a 2 h incubation at 37˚C, the resulting formazan crystals were dissolved in 150 μl of DMSO, and absorbance was measured at 570 nm using a microplate reader (INNO; L-Tek, Seongnam, Republic of Korea). Cytotoxicity was evaluated using the LDH Plus Cytotoxicity Assay Kit (GBL-P500; Dyne Bio, Seongnam, Republic of Korea) according to the manufacturer's instructions, and absorbance was measured at 490 nm.

Flow cytometric analysis of apoptosis. Apoptotic cell death was analyzed using a Muse Annexin V & Dead Cell Kit (MCH100105; Cytek Biosciences, Fremont, CA, USA) according to the manufacturer's guidelines. Cells were seeded in six-well plates at a density of $5x10^4$ cells/well and allowed to adhere for 24 h before treatment with different concentrations of TAK-981 for 48 h. After incubation, both floating and adherent cells were collected by trypsinization, centrifuged, and resuspended in 100 μl of assay medium. Subsequently, 100 μl of Annexin V & Dead Cell Reagent containing 7-AAD was added, and the mixture was incubated for 20 min at room temperature in the dark. Stained samples were immediately analyzed using a Guava Muse Cell Analyzer (0500-3115; Luminex, Austin, TX, USA).

Flow cytometric analysis of cell cycle progression. The distribution of cells across different cell cycle phases was determined using the Muse Cell Cycle Kit (MCH100106; Cytek Biosciences, Fremont, CA, USA). Briefly, the cells were harvested, washed with PBS, and fixed with 70% cold ethanol at -20˚C for approximately 3 h. After fixation, the samples were centrifuged, resuspended in 200 μl of Muse Cell Cycle Reagent, and incubated for 30 min at room temperature in the dark. DNA content was analyzed using a Guava Muse Cell Analyzer to determine the percentage of cells in the G_0/G_1, S and G_2/M phases.

Flow cytometric analysis of Ki67-positive cells. Cell proliferation was assessed using the Muse Ki67 Proliferation Kit (MCH100114; Cytek Biosciences, Fremont, CA, USA). After treatment, cells were collected and processed for fixation and permeabilization according to the manufacturer's protocol. The cells were then stained with either an anti-Ki67 antibody or the corresponding isotype control antibody. Ki67-positive populations were quantified using a Guava Muse Cell Analyzer.

Flow cytometric analysis of intracellular ROS. Intracellular ROS levels were quantified using the Muse Oxidative Stress Kit (MCH100111; Cytek Biosciences) following the manufacturer's protocol. Cells were seeded in six-well plates at a density of $5x10^4$ cells per well and allowed to attach for 24 h before exposure to TAK-981 at concentrations of 0, 0.5, 1, or 2 μM for 48 h. After incubation, the cells were collected, washed, and resuspended in 1X assay buffer. Afterward, cell suspensions were stained with the Muse Oxidative Stress Reagent and incubated at 37˚C for 30 min in the dark. ROS generation was analyzed using a Guava Muse Cell Analyzer.

Measurement of mitochondrial membrane potential ($\Delta\Psi m$). $\Delta\Psi m$ was evaluated using the Muse MitoPotential Kit (MCH100110; Cytek Biosciences) according to the manufacturer's instructions. After 48 h of TAK-981 treatment, the cells were harvested, washed with PBS, and resuspended in 1X assay buffer at a concentration of $1\text{-}2x10^6$ cells/ml. Next, the cells were stained with MitoPotential dye working solution for 20-30 min at room temperature in the dark, followed by staining with 7-AAD for an additional 5 min. The samples were analyzed using a Guava Muse Cell Analyzer, and the percentages of live/depolarized, total depolarized, and live/polarized cells were quantified.

Flow cytometric analysis of autophagy. Autophagic activity was analyzed using the Muse Autophagy LC3 Antibody-Based Kit (MCH200109; Cytek Biosciences) in accordance with the manufacturer's instructions. Briefly, both control and TAK-981-treated cells were collected, washed, and incubated with anti-LC3 Alexa Fluor 555 antibody and 1X autophagy reagent for 30 min in the dark. After staining, the cells were resuspended in 200 μl of 1X assay buffer and subjected to flow cytometric analysis using a Guava Muse Cell Analyzer. The degree of autophagy induction was determined by comparing the fluorescence signal intensities of treated and untreated samples.

Protein extraction and western blotting. Total cellular proteins were isolated using radio-immunoprecipitation assay lysis buffer (R2002; Biosesang, Gyeonggi-do, Republic of Korea) supplemented with a protease inhibitor cocktail (04693132001; Roche, Basel, Switzerland). Protein samples were separated using 15% sodium dodecyl sulphate-polyacrylamide gel electrophoresis and transferred onto polyvinylidene fluoride membranes (IPVH00010; Merck Millipore, Billerica, MA, USA). The membranes were blocked with 5% skim milk (262100; BD Difco, Franklin Lakes, NJ, USA) for 1 h at room temperature and incubated overnight at 4˚C with primary antibodies. The following primary antibodies were used: SUMO2/3 (4971T), SAE2 (8688T), poly (ADP-ribose) polymerase (PARP; 9542S), caspase-3 (9665S), cleaved caspase-3 (9664S), p53 (2527S), p27 (3686T), p21 (2947S), p62/SQSTM1 (5114T), LC3B (2775S), and β-actin (4967S) (all from Cell Signaling Technology, Danvers, MA, USA), as well as SAE1 (sc-398080) from Santa Cruz Biotechnology (Dallas, TX, USA). After washing, the membranes were incubated with horseradish peroxidase (HRP)-conjugated secondary antibodies (7074S or 7076S; Cell Signaling Technology) for 1 h. Immunoreactive bands were visualized using the Western Pico ECL Kit (PICO-250; LPS Solution, Daejeon, Republic of Korea) and detected using an Azure c280 imaging system (Azure Biosystems; Dublin, CA, USA).

Statistical analysis. Statistical analyses were conducted using GraphPad Prism software (version 8.0; GraphPad Software, La Jolla, CA, USA). All data are expressed as the mean ± standard deviation obtained from at least three independent experiments. Group comparisons were conducted using one-way analysis of variance, followed by Tukey's multiple comparisons test or Dunnett's post hoc test, when appropriate. $P<0.05$ was considered to indicate a statistically significant difference.

Results

TAK-981 exhibits stronger cytotoxic effects in SK-UT-1B than in SK-UT-1 cells. The cytotoxic effect of TAK-981 on Ut-LMS cells was evaluated, in which SK-UT-1B cells were treated with increasing concentrations of TAK-981 (0, 0.25, 0.5, 1, and 2 μM) for 24 and 48 h, and cell viability was measured using the MTT assay. After 24 h of treatment, TAK-981 displayed minimal cytotoxicity, with 2 μM treatment maintaining 82.5% cell viability compared to the control. In contrast, prolonged exposure for 48 h markedly reduced cell viability, showing 66.7, 38.1, 31.7, and 33.5% viability at 0.25, 0.5, 1, and 2 μM, respectively (Fig. 1A). Consistent with these findings, LDH release, an indicator of membrane integrity loss, demonstrated no marked change at 24 h but increased substantially after 48 h, with an approximately 2.8-fold elevation at 1 and 2 μM compared to the control (Fig. 1B).

Other Ut-LMS cell lines (SK-UT-1) exhibited no marked changes in viability after 48 h of TAK-981 exposure at similar concentrations (Fig. 1C). SK-UT-1 cells exhibited <5% viability only at extremely high concentrations (up to 100 μM), indicating nonspecific cytotoxicity at supra-physiological levels (Fig. 1D). Collectively, these results demonstrate that TAK-981 exerted markedly greater cytotoxicity in SK-UT-1B cells than in SK-UT-1 cells, particularly at low micromolar concentrations and with prolonged exposure. Because normal uterine smooth muscle cells have been reported to show reduced viability only at TAK-981 concentrations ≥50 μM (17), SK-UT-1B cells were selected as the primary model for subsequent mechanistic analyses.

TAK-981 induces apoptosis in SK-UT-1B cells. Whether the cytotoxic effect of TAK-981 was associated with apoptosis was determined using Annexin V staining followed by flow cytometric analysis in SK-UT-1B cells after 48 h of treatment. The proportion of apoptotic cells progressively increased with the concentration of TAK-981, from 7.7% in control cells to 19.9, 31.0, and 31.7% in cells treated with 0.5, 1, and 2 μM, respectively (Fig. 1E). TAK-981 induced apoptosis in SK-UT-1B cells and this apoptotic effect became more prominent at higher drug concentrations.

TAK-981 induces G_0/G_1-phase cell-cycle arrest and suppresses proliferation in SK-UT-1B cells. The anti-proliferative effect of TAK-981 were investigated by analyzing the cell cycle distribution and proliferation markers in SK-UT-1B cells after 48 h of treatment. Flow cytometry analysis indicated that TAK-981 caused a marked accumulation of cells in the G_0/G_1 phase (Fig. 2A). The proportion of G_0/G_1-phase cells increased from 59.7% in control cells to 76.7, 78.6, and 78.3% following exposure to 0.5, 1, and 2 μM TAK-981, respectively, whereas the proportion of G_2/M-phase cells decreased from 23.4% in control cells to approximately 15% after treatment.

Cell proliferation was evaluated by assessing Ki67 expression using flow cytometry. The proportion of Ki67-positive SK-UT-1B cells decreased markedly following TAK-981 exposure, from 90.7% in control cells to 64.5, 50.4, and 48.1% after treatment with 0.5, 1, and 2 μM, respectively (Fig. 2B). Thus, TAK-981 suppressed DNA synthesis and the proliferation of SK-UT-1B cells by inducing G_0/G_1-phase cell-cycle arrest. Together with the apoptosis data, these findings suggest that TAK-981 inhibited SK-UT-1B cell growth through coordinated suppression of proliferation and induction of apoptotic cell death.

TAK-981-induced apoptosis is associated with ROS accumulation and mitochondrial dysfunction in SK-UT-1B cells. Whether oxidative stress contributed to TAK-981-induced cytotoxicity was determined by treating SK-UT-1B cells with TAK-981 (0.5-2 μM) for 48 h, and intracellular ROS levels were measured using a fluorescent detection assay followed by flow cytometric analysis. TAK-981 treatment markedly

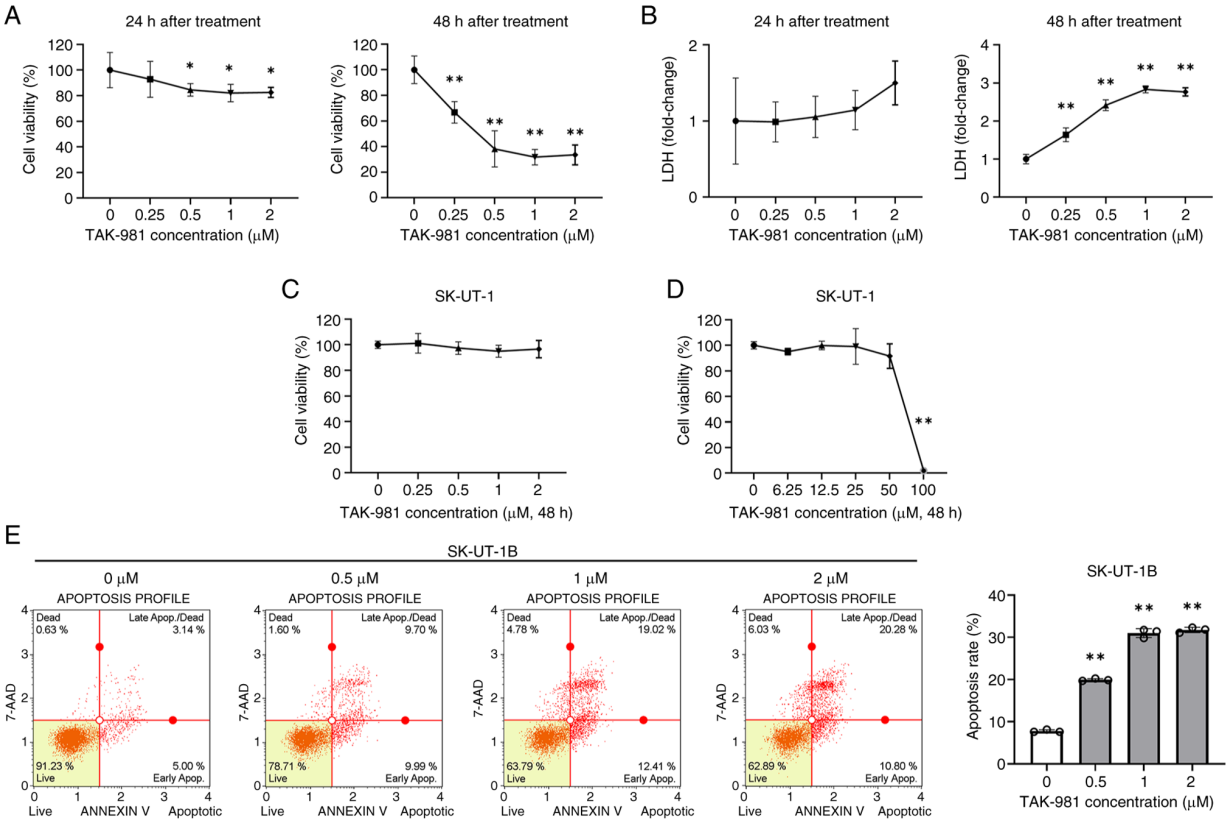

Figure 1. Cytotoxic and apoptotic effects of TAK-981 on SK-UT-1B cells (A) SK-UT-1B cells were treated with increasing concentrations of TAK-981 (0-2 μM) for 24 and 48 h, and cell viability was quantified using the MTT assay. Viability is presented as a percentage relative to the untreated control. (B) LDH release, an indicator of membrane damage, was measured after 24 and 48 h of TAK-981 exposure. (C) SK-UT-1 cells were treated with TAK-981 at the same concentrations for 48 h, and cell viability was assessed using the MTT assay. (D) SK-UT-1 cells were treated with higher concentrations of TAK-981, up to 100 μM, for 48 h, and cell viability was assessed using the MTT assay. (E) Annexin V flow-cytometric analysis showing increased apoptotic populations following 48 h of TAK-981 treatment. Data are presented as mean ± standard deviation from three independent experiments. The LDH assay was performed using six replicates per group. *P<0.05, **P<0.01 vs. control. LDH, lactate dehydrogenase.

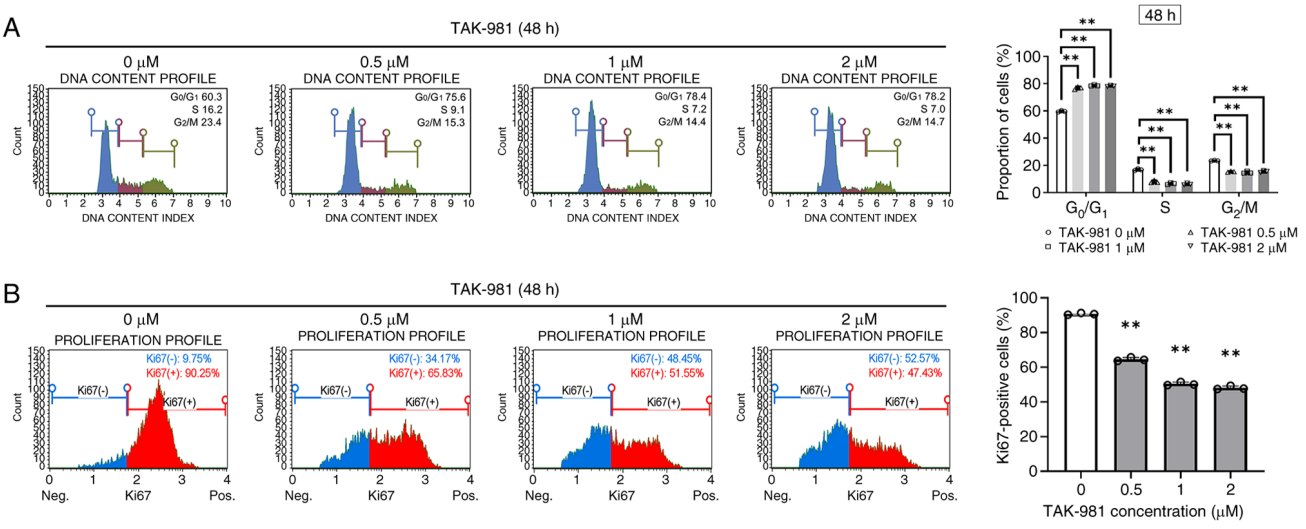

Figure 2. TAK-981 induces G_0/G_1-phase arrest and inhibits cell proliferation in SK-UT-1B cells (A) SK-UT-1B cells were treated with increasing concentrations of TAK-981 (0-2 μM) for 48 h, and cell-cycle distribution was analyzed using flow cytometry. The proportions of cells in the G_0/G_1, S and G_2/M phases were quantified. (B) Proliferating and nonproliferating cell populations were measured using the Muse Ki67 Proliferation Kit based on Ki67 expression. Data are presented as the mean ± standard deviation from three independent experiments. **P<0.01 vs. control.

increased the proportion of ROS-positive cells from 2.0% in the control group to 12.6, 18.0, and 23.0% at 0.5, 1, and 2 μM, respectively (Fig. 3A).

Mitochondrial membrane potential ($\Delta\Psi$m) was evaluated using the Muse MitoPotential assay after 48 h of TAK-981 exposure. The proportion of total depolarized SK-UT-1B

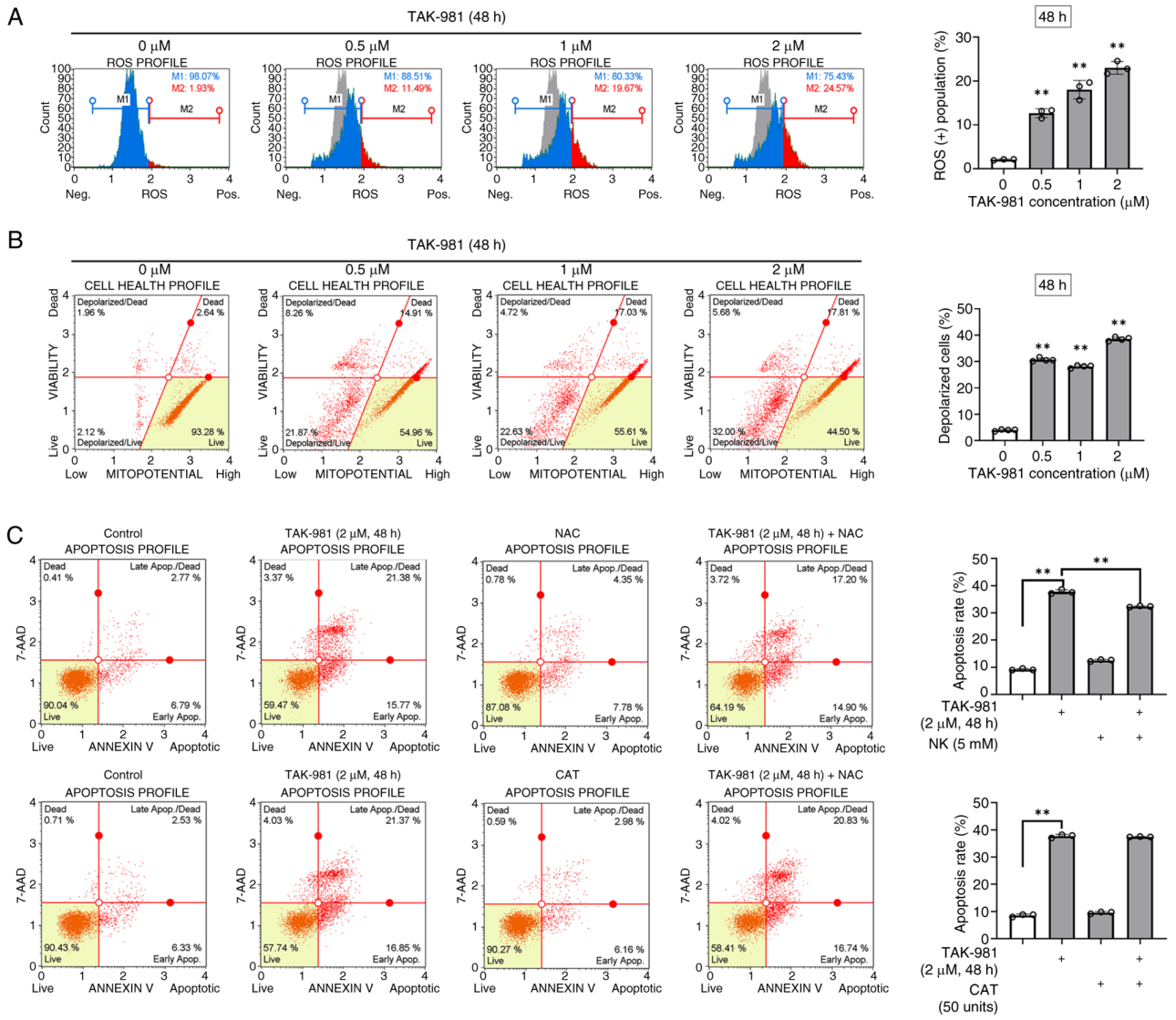

Figure 3. TAK-981 induces oxidative stress and mitochondrial dysfunction in SK-UT-1B cells (A) Intracellular ROS generation was analyzed in SK-UT-1B cells using a ROS-sensitive fluorescent probe followed by flow cytometric analysis after 48 h of TAK-981 (0-2 μM) treatment. (B) Mitochondrial membrane potential was assessed using the Muse MitoPotential Kit after 48 h of TAK-981 exposure. Representative dot plots and quantitative analyses are shown. (C) Apoptosis was analyzed in SK-UT-1B cells treated with 2 μM TAK-981 for 48 h in the presence or absence of the ROS scavengers, NAC (5 mM) and CAT (50 units). Data are presented as mean ± standard deviation from three independent experiments. **P<0.01 vs. control. CAT, catalase; NAC, N-acetyl-L-cysteine; ROS, reactive oxygen species.

cells increased from 3.96% in the control group to 30.6, 28.1, and 38.5% after treatment with 0.5, 1, and 2 μM TAK-981, respectively (Fig. 3B). SK-UT-1B cells were co-treated with the antioxidants, NAC or CAT, for 48 h in the presence of 2 μM TAK-981 to verify whether ROS accumulation mediated TAK-981-induced apoptosis. NAC markedly reduced the TAK-981-induced apoptosis, whereas CAT exerted little effect (Fig. 3C). These results indicate that TAK-981 increased ROS accumulation and mitochondrial membrane depolarization in SK-UT-1B cells; ROS contributed, at least in part, to TAK-981-induced apoptotic cell death.

TAK-981 inhibits SUMOylation without altering SAE1/SAE2 expression and modulates apoptotic and cell-cycle regulators in SK-UT-1B cells. TAK-981 inhibits SUMOylation by blocking SAE2 activity without altering protein levels (10). The expression of SUMO2/3-conjugated proteins, SAE1 and SAE2, was analyzed using western blotting to examine whether TAK-981 affected SUMO pathway-related proteins in SK-UT-1B cells. After 48 h of treatment with 0.5-2 μM TAK-981, SUMO-conjugated proteins were markedly reduced, whereas SAE1 and SAE2 protein levels were unchanged (Fig. 4A). These findings suggest that TAK-981 suppressed SUMOylation primarily through functional inhibition rather than through changes in SAE enzyme expression.

The expression of caspase-3, cleaved caspase-3, and PARP was analyzed to investigate the apoptosis-related signaling events. TAK-981 treatment enhanced caspase-3 and PARP cleavage after 48 h, indicating the activation of apoptotic signaling in SK-UT-1B cells (Fig. 4B). The downstream mechanisms associated with TAK-981-mediated growth suppression were determined by examining the expression of key cell cycle regulators. Western blotting indicated that TAK-981 markedly increased p53 and p21 protein expression

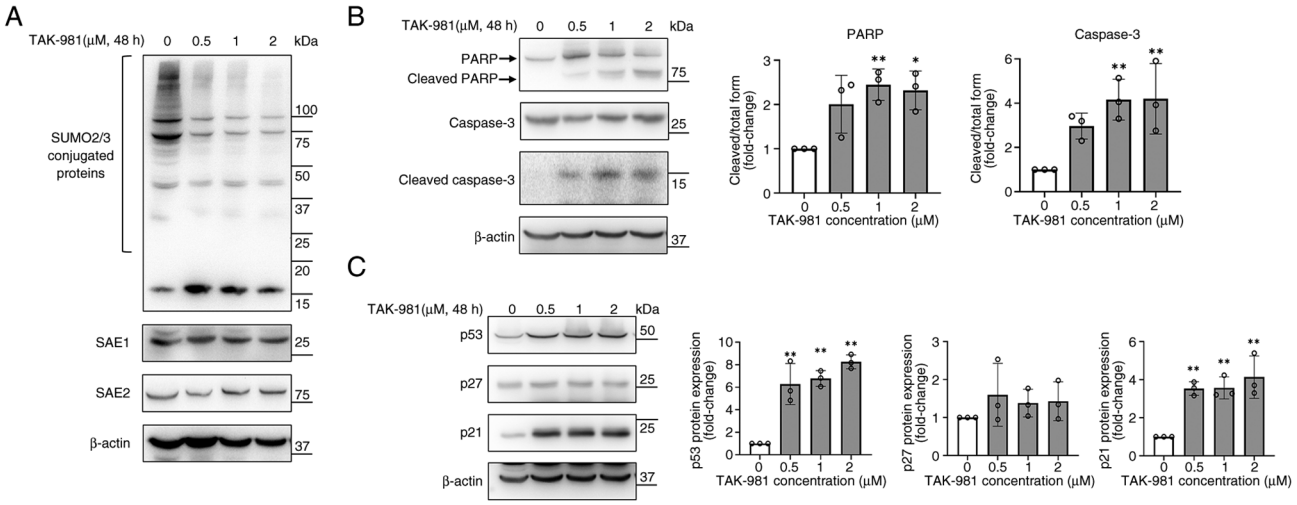

Figure 4. TAK-981 inhibits SUMOylation and modulates apoptotic- and cell-cycle-related pathways in SK-UT-1B cells (A) SK-UT-1B cells were treated with TAK-981 (0.5, 1, and 2 μM) for 48 h, and the expression of SUMO2/3, SAE1, and SAE2 was analyzed using western blotting with β-actin as a loading control. (B) Apoptosis-associated proteins, including PARP, caspase-3 and cleaved caspase-3, were analyzed using western blotting in SK-UT-1B cells following 48 h of TAK-981 treatment. Semi-quantified band intensities are shown in the right panels with β-actin serving as a loading control. (C) Cell cycle-associated proteins, including p53, p27 and p21, were analyzed using western blotting in SK-UT-1B cells following 48 h of TAK-981 treatment. Semi-quantified band intensities are shown in the right panels with β-actin serving as a loading control. Data represent mean ± standard deviation from three independent experiments. *P<0.05, **P<0.01 vs. control. PARP, poly (ADP-ribose) polymerase; SAE, SUMO-activating enzyme; SUMO, small ubiquitin-like modifier.

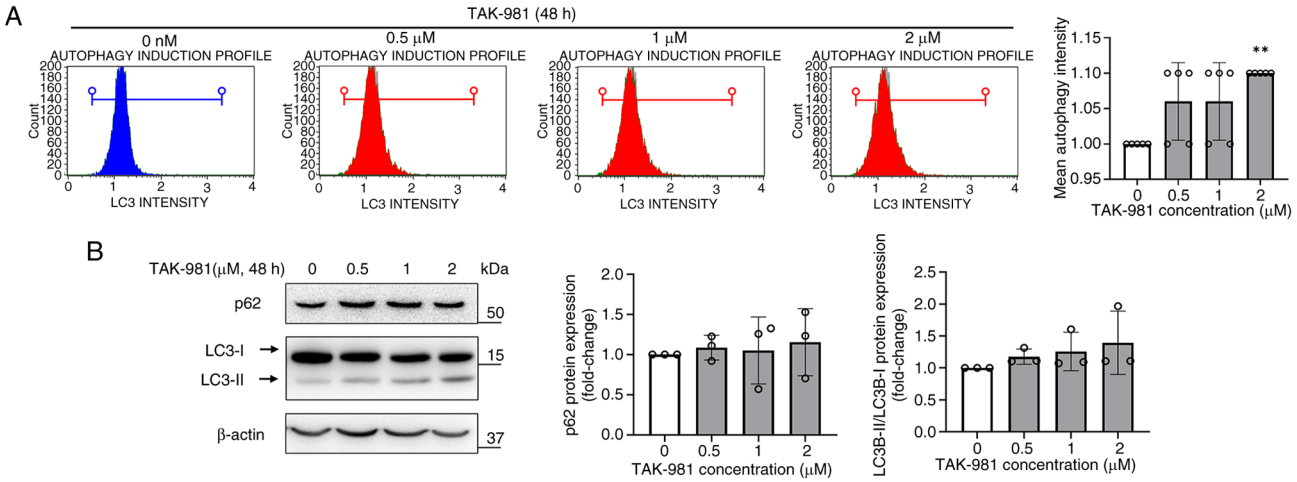

Figure 5. TAK-981 does not modulate autophagy in SK-UT-1B cells (A) Flow cytometric analysis of LC3 protein levels in SK-UT-1B cells treated with TAK-981 (0.5, 1, and 2 μM) for 48 h. After treatment, cells were stained with an anti-LC3 antibody, and the percentage of LC3-positive cells was quantified to assess autophagy induction. (B) Western blotting of p62 and LC3 expression in SK-UT-1B cells following treatment with TAK-981 (0.5, 1, and 2 μM) for 48 h. Protein levels of p62, LC3-I and LC3-II were determined, with β-actin used as a loading control. Band intensities are shown in the right panel. Data are presented as mean ± standard deviation from three independent experiments. **P<0.01 vs. control.

after 48 h of treatment, whereas p27 levels were unchanged in SK-UT-1B cells (Fig. 4C). Collectively, these findings indicate that TAK-981 inhibited SUMOylation, increased p53 and p21 protein expression, and triggered apoptotic signaling cascades in SK-UT-1B cells.

TAK-981 does not significantly modulate autophagy in SK-UT-1B cells. Autophagy plays a key role in maintaining cell survival and homeostasis under normal and stressful conditions. Whether TAK-981 affected autophagy in SK-UT-1B cells was investigated by measuring LC3B expression by flow cytometry after treatment with 0.5, 1, or 2 μM TAK-981 for 48 h. TAK-981 treatment did not alter LC3B fluorescence intensity markedly at most concentrations, although a slight increase was observed at 2 μM (Fig. 5A). Consistent with this, western blotting indicated no marked changes in LC3B-I/II conversion or p62 expression after 48 h of TAK-981 treatment (Fig. 5B). TAK-981 therefore did not modulate autophagy in SK-UT-1B cells, suggesting that its cytotoxic effects were largely independent of the autophagic pathway.

Discussion

This study provides the first evidence that the SUMO inhibitor TAK-981 suppressed the viability of SK-UT-1B cells, even at low concentrations, and was associated with ROS accumulation,

mitochondrial membrane depolarization, apoptosis, and G_0/G_1 cell cycle arrest, accompanied by the activation of p21 and p53. These results suggest that TAK-981 disrupts Ut-LMS cell survival by simultaneously engaging in ROS-dependent apoptotic signaling and SUMO-inhibition-mediated transcriptional pathways.

The present study extends our previous findings in ELT3 uterine leiomyoma cells to a malignant Ut-LMS cell model (17). Despite their shared uterine smooth muscle origin, TAK-981-associated cellular responses differed between benign leiomyoma and malignant Ut-LMS cells. TAK-981 increased ROS accumulation in both ELT3 and SK-UT-1B cells; however, apoptosis appeared to be ROS-independent in ELT3 cells, whereas ROS-associated mitochondrial dysfunction was more closely linked to apoptosis in SK-UT-1B cells. In addition, TAK-981 was associated with G_2/M arrest, MEK/ERK inhibition, reduced extracellular matrix-related protein expression, and autophagy-related changes in ELT3 cells, whereas it was associated with G_0/G_1 arrest and p53/p21 activation in SK-UT-1B cells. These differences suggest that cellular responses to TAK-981 may depend on tumor type and cellular context, and further studies are needed to clarify these model-dependent effects.

Post-translational modification mechanisms have emerged as critical determinants of tumor survival, proliferation, and therapeutic resistance (18-20). Of these, the SUMO pathway has gained particular attention as a key regulatory axis that governs essential cellular processes, such as DNA damage repair, cell-cycle progression, stress responses, transcriptional regulation, and protein stability, which are tightly linked to tumor growth and progression (13,21). Aberrant SUMOylation has been reported to promote malignant transformation, cancer stemness, drug resistance, and metastasis in multiple tumor types (11,13,22). Consistent with these determinations, the current study showed that TAK-981 markedly inhibited global SUMOylation in SK-UT-1B cells and affected multiple cellular processes, including reduced cell viability, G_0/G_1 cell-cycle arrest, ROS accumulation, mitochondrial dysfunction, and apoptosis. Pharmacological inhibition of the SUMO cascade, particularly through SAE inhibition by TAK-981, may therefore represent a promising therapeutic strategy for Ut-LMS (14,15,17).

A notable aspect of the findings was the differential sensitivity of Ut-LMS cell lines. SK-UT-1B cells exhibited marked susceptibility to low micromolar concentrations of TAK-981, whereas SK-UT-1 cells demonstrated limited responses at similar concentrations. Several biological factors may be responsible for this variability. Although SK-UT-1B is a sub-line derived from the parental SK-UT-1 cell line, it displays distinct molecular characteristics, including a potentially wild-type p53 background compared to the p53-mutant status reported for SK-UT-1 (23-25). As the p53 status influences cell cycle regulation, DNA damage responses, and oxidative stress sensitivity (26-28), TAK-981-induced p21/p53 activation may exert greater biological effects on SK-UT-1B cells. Based on our findings, the higher sensitivity of SK-UT-1B cells to TAK-981 may be related to their greater dependence on SUMOylation-associated stress-adaptive mechanisms and their susceptibility to p53/p21-mediated cell-cycle arrest and ROS-associated mitochondrial apoptosis. In contrast, SK-UT-1 cells may possess distinct molecular features that confer relative resistance to TAK-981, such as altered p53 pathway activity, reduced SUMO pathway dependency, or increased tolerance to oxidative and mitochondrial stress. These intrinsic differences highlight the significance of molecular heterogeneity in Ut-LMS cells and underscore the need to tailor targeted therapies based on the tumor genotype and pathway dependency.

Compared with conventional agents, such as doxorubicin, gemcitabine, or docetaxel, which generally exert nonspecific cytotoxic effects, TAK-981 is highly specific as it directly inhibits the SUMOylation machinery (29). This provides a novel therapeutic approach for Ut-LMS, particularly because SUMO-dependent transcriptional and stress response pathways are increasingly recognized as actionable vulnerabilities in high-grade sarcomas. The robust cytotoxicity observed in SK-UT-1B cells at pharmacologically-relevant concentrations supports the existence of a therapeutic window that distinguishes TAK-981 from traditional chemotherapeutics that often damage malignant and healthy tissues.

From a translational perspective, the SUMO pathway inhibition may offer opportunities for precision-guided Ut-LMS therapy. The molecular diversity observed between SK-UT-1B and SK-UT-1 cells suggests that biomarkers, such as p53 functionality, SUMO pathway dependency, and ROS-related gene signatures, could serve to stratify patients most likely to benefit from TAK-981. Furthermore, combining SUMO inhibition with agents targeting DNA damage repair, oxidative stress pathways, or immune activation may enhance therapeutic responses due to the known role of TAK-981 in amplifying type I interferon signaling (9,10).

This study had several limitations. These findings are based solely on *in vitro* experiments, and additional *in vivo* validation using animal models or patient-derived xenografts is required to confirm the therapeutic potential of TAK-981. Furthermore, the molecular factors underlying the differential sensitivity among Ut-LMS cell lines warrant comprehensive investigation through genomic, transcriptomic, and proteomic analyses.

In conclusion, the findings provide the first evidence that TAK-981 exerts strong anti-proliferative and pro-apoptotic effects in SK-UT-1B cells. These effects were associated with SUMOylation inhibition, ROS accumulation, mitochondrial dysfunction, G_0/G_1 cell-cycle arrest, and activation of p53/p21 and apoptotic signaling. These data highlight TAK-981 as a promising candidate for future therapeutic development and support the broader concept of targeting SUMOylation as an emerging strategy for the treatment of aggressive Ut-LMS.

Acknowledgements

No applicable.

Funding

This work was supported by a research fund from Chosun University, 2025 (grant no. K208554004).

Availability of data and materials

The data generated in the present study may be requested from the corresponding author.

Authors' contributions

HJ and HL designed the experiments and revised the manuscript. HJ conducted experiments and wrote the manuscript. HJ and HL conducted the data analysis. HJ and HL confirm the authenticity of all the raw data. Both authors read and approved the final manuscript.

Ethics approval and consent to participate

Not applicable.

Patient consent for publication

Not applicable.

Competing interests

The authors declare that they have no competing interests.

References

1. Bogani G, Caruso G, Ray-Coquard I, Ramirez PT, Concin N, Ngoi NY, Coleman RL, Mariani A, Cliby W, Leitao MM, *et al*: Uterine leiomyosarcoma. Int J Gynecol Cancer 35: 101992, 2025.
2. Khamaiseh S, Koivisto-Korander R, Schreiber N, Pitkanen E, Ahvenainen T, Butzow R, Mehine M and Vahteristo P: Transcriptome profiling of uterine leiomyosarcomas identifies a leiomyoma-like expression pattern that indicates better survival. BJC Rep 3: 76, 2025.
3. Yang Q, Madueke-Laveaux OS, Cun H, Wlodarczyk M, Garcia N, Carvalho KC and Al-Hendy A: Comprehensive review of uterine leiomyosarcoma: pathogenesis, diagnosis, prognosis, and targeted therapy. Cells 13: 1106, 2024.
4. Henry T, Fabre E, Baccar LS and Lamuraglia M: Longer survival in patients with metastatic uterine leiomyosarcoma treated with trabectedin: A case report. Mol Clin Oncol 10: 387-390, 2019.
5. Gupta AA, Yao X, Verma S, Mackay H, Hopkins L; Sarcoma Disease Site Group and the Gynecology Cancer Disease Site Group: Systematic chemotherapy for inoperable, locally advanced, recurrent, or metastatic uterine leiomyosarcoma: A systematic review. Clin Oncol (R Coll Radiol) 25: 346-355, 2013.
6. Sparic R, Andjic M, Babovic I, Nejkovic L, Mitrovic M, Stulic J, Pupovac M and Tinelli A: Molecular insights in uterine leiomyosarcoma: A systematic review. Int J Mol Sci 23: 9728, 2022.
7. Chudasama P, Mughal SS, Sanders MA, Hubschmann D, Chung I, Deeg KI, Wong SH, Rabe S, Hlevnjak M, Zapatka M, *et al*: Integrative genomic and transcriptomic analysis of leiomyosarcoma. Nat Commun 9: 144, 2018.
8. Dall GV, Hamilton A, Ratnayake G, Scott C and Barker H: Interrogating the genomic landscape of uterine leiomyosarcoma: A potential for patient benefit. Cancers (Basel) 14: 1561, 2022.
9. Langston SP, Grossman S, England D, Afroze R, Bence N, Bowman D, Bump N, Chau R, Chuang BC, Claiborne C, *et al*: Discovery of TAK-981, a first-in-class inhibitor of SUMO-activating enzyme for the treatment of cancer. J Med Chem 64: 2501-2520, 2021.
10. Lightcap ES, Yu P, Grossman S, Song K, Khattar M, Xega K, He X, Gavin JM, Imaichi H, Garnsey JJ, *et al*: A small-molecule SUMOylation inhibitor activates antitumor immune responses and potentiates immune therapies in preclinical models. Sci Transl Med 13: eaba7791, 2021.
11. Gu Y, Fang Y, Wu X, Xu T, Hu T, Xu Y, Ma P, Wang Q and Shu Y: The emerging roles of SUMOylation in the tumor microenvironment and therapeutic implications. Exp Hematol Oncol 12: 58, 2023.
12. Eifler K and Vertegaal ACO: SUMOylation-mediated regulation of cell cycle progression and cancer. Trends Biochem Sci 40: 779-793, 2015.
13. Han ZJ, Feng YH, Gu BH, Li YM and Chen H: The post-translational modification, SUMOylation, and cancer (Review). Int J Oncol 52: 1081-1094, 2018.
14. Kumar S, Schoonderwoerd MJA, Kroonen JS, de Graaf IJ, Sluijter M, Ruano D, Gonzalez-Prieto R, Verlaan-de Vries M, Rip J, Arens R, *et al*: Targeting pancreatic cancer by TAK-981: A SUMOylation inhibitor that activates the immune system and blocks cancer cell cycle progression in a preclinical model. Gut 71: 2266-2283, 2022.
15. Kim HS, Kim BR, Dao TTP, Kim JM, Kim YJ, Son H, Jo S, Kim D, Kim J, Suh YJ, *et al*: TAK-981, a SUMOylation inhibitor, suppresses AML growth immune-independently. Blood Adv 7: 3155-3168, 2023.
16. Zhou H, Deng N, Li Y, Hu X, Yu X, Jia S, Zheng C, Gao S, Wu H and Li K: Distinctive tumorigenic significance and innovative oncology targets of SUMOylation. Theranostics 14: 3127-3149, 2024.
17. Liu H, Seo S and Joung H: TAK-981 enhances antitumor activity in ELT3 uterine leiomyoma cells through the modulation of apoptosis, cell cycle arrest, and autophagy. Biochem Biophys Res Commun 770: 152000, 2025.
18. Bruno PS, Arshad A, Gogu MR, Waterman N, Flack R, Dunn K, Darie CC and Neagu AN: Post-translational modifications of proteins orchestrate all hallmarks of cancer. Life (Basel) 15: 126, 2025.
19. Dutta H and Jain N: Post-translational modifications and their implications in cancer. Front Oncol 13: 1240115, 2023.
20. Li W, Li F, Zhang X, Lin HK and Xu C: Insights into the post-translational modification and its emerging role in shaping the tumor microenvironment. Signal Transduct Target Ther 6: 422, 2021.
21. Kroonen JS and Vertegaal ACO: Targeting SUMO signaling to wrestle cancer. Trends Cancer 7: 496-510, 2021.
22. Kukkula A, Ojala VK, Mendez LM, Sistonen L, Elenius K and Sundvall M: Therapeutic potential of targeting the SUMO pathway in cancer. Cancers (Basel) 13: 4402, 2021.
23. Joung H, Seo S and Liu H: MG132 induces cell type-specific anticancer effects in uterine leiomyosarcoma cell lines. Mol Med Rep 31: 2025.
24. Smardova J, Pavlova S, Svitakova M, Grochova D and Ravcukova B: Analysis of p53 status in human cell lines using a functional assay in yeast: Detection of new non-sense p53 mutation in codon 124. Oncol Rep 14: 901-907, 2005.
25. Coley HM, Shotton CF, Kokkinos MI and Thomas H: The effects of the CDK inhibitor seliciclib alone or in combination with cisplatin in human uterine sarcoma cell lines. Gynecol Oncol 105: 462-469, 2007.
26. Pitolli C, Wang Y, Candi E, Shi Y, Melino G and Amelio I: p53-mediated tumor suppression: DNA-damage response and alternative mechanisms. Cancers (Basel) 11: 1983, 2019.
27. Beyfuss K and Hood DA: A systematic review of p53 regulation of oxidative stress in skeletal muscle. Redox Rep 23: 100-117, 2018.
28. Vousden KH and Prives C: Blinded by the light: The growing complexity of p53. Cell 137: 413-431, 2009.
29. Kroonen JS, de Graaf IJ, Kumar S, Remst DFG, Wouters AK, Heemskerk MHM and Vertegaal ACO: Inhibition of SUMOylation enhances DNA hypomethylating drug efficacy to reduce outgrowth of hematopoietic malignancies. Leukemia 37: 864-876, 2023.